Abstract

Janus Nanoparticles are amphiphilic molecules with several applications in biology. With several associated innovative and cutting-edge technologies proposed over the last few decades, they are of particular interest in fields such as cancer diagnosis and therapy. The goal of this project is to implement some dissipative particles dynamics simulations of a Janus nanoparticles-based magnetolytic cancer therapy. The advantage of such treatment could range from the low-toxicity, easy manipulation, precise targeting and precise cellular killing activation through the application of a very localized magnetic field. Since now, only empirical data existed, with a lack of computational analyses allowing to investigate whether a magneto-mechanical "bombardment" of cancer cells membranes with Janus nanoparticles could be sufficient on its own to induce cellular death. If it is the case, which would be the best parameters maximizing the membrane disruption? The simulations performed here show not only that this mechanism is sufficient to disrupt the membrane integrity but also provide the optimal parameters to achieve a maximal destruction.

Introduction

In the last decades, a great number of therapies has been developed to fight cancer. Nowadays, multiple treatments options exist, including for example immunotherapy, radiotherapy, chemotherapy, surgery. The choice of the right therapy is fundamental to efficiently fight a specific type of tumor. Despite the diversity of available options, one main issue regarding the possible off-side drawbacks of those techniques still persists. With the development of cutting-edge personalized treatments the field of oncoengineering tries to reduce those problematics. Because of the extremely high cost and complexity of some new technologies, it is however urgent to also explore and test alternative solutions that locally target tissues with a low level of side effects. Exploiting the modern simulation techniques could be an efficient and innovative approach taking advantage of the power and cheapness of the in-silico methods to predict some effects that can then be confirmed with some in-vitro assays. This principle has been extensively applied for example in the field of drug discovery, to speed up the entire development process and reduce the cost of the initial phases, by reducing the amount of in-vitro necessary tests. With this general idea, the goal of this short report is to propose a simulation approach to investigate an already in-vitro tested cancer therapy. The aim is to find out if an optimal set-up maximizing the treatment efficacy can be established. This could be the basis for further in-vitro and in-vivo targeted and precise investigations, allowing to avoid the testing of a very large number of the therapy parameters combinations.

The so-called magnetolytic therapy studied here is a very interesting example of innovative cancer therapy and was first proposed by *Hu et al.*¹ in 2010. Specifically-engineered Janus Nanoparticles (JNPs) are used.

Janus Nanoparticles (JNPs), as the name suggests, are asymmetric amphiphilic particles with several applications in biology and electronics. Compared to other heterogeneous physical systems they present several advantages such as the absence of alteration of the single components physical properties, typically present for example in heterogeneous nanocrystals. This possibility to combine several different or in some cases incompatible mechanical, physical and chemical properties offers a great flexibility and potential.

Specific examples of JNPs include the engineering of magnetic-hemispheres complemented with a second special drug-delivery nonporous² or cell-specific hemisphere^{3,1}. This offers several interesting properties in cancer diagnosis or therapy. The presence of a magnetic domain allows in fact to efficiently target tumor tissues by enhancing the enhanced permeability and retention (EPR) effect, defined in this case as the particularly high accumulation of nanoparticles in the tumorigenic tissues. In addition to the natural EPR effect associated to nano-macromolecules⁴, a magnetic field can in fact be exploited to guide and retain them locally and precisely. A very deep tissue penetration can be achieved.

A similar approach to the magnetolytic therapy proposed in the reference paper of *Hu et al.*¹ was previously presented by *Kim et al.*⁵ Ferromagnetic cancer-cells specific and Ab-coated microdiscs were used instead of Janus nanoparticles. Results showed that a short in-vitro application (10 min) of a low-intensity and low-frequency (few tens of Oe, few tens of Hz) spinning magnetic field is sufficient to achieve ~90% of cancer cells magnetomechanical destruction, independently to an hyperthermia mechanism. This is possible thanks to an induced rotation of the disks, interfering with the cellular membrane. This astonishing efficacy was obtained using disks with a diameter of 1µm and a total thickness of 70 nm. The increasing in the frequency of the oscillating magnetic field revealed-out to be inefficient, with a decrease in the fraction of the killed cancer cells. The authors explained this behavior with the incapacity of the magnetic disks to respond to the rapidly oscillating magnetic field, resulting in an incapacity of disrupting the cell membranes

integrity. Interestingly, the in-vitro assays allowed to conclude that the loss of membrane integrity was not exclusively caused by the force applied by the spinning magnetic disks. In fact, the delivered force (in the order of a few tens of pN) cannot be compared to the few-hundreds pN needed to disrupt it. It was therefore concluded that the observed effects were caused by the activation of some intrinsic cell-death pathways.

In this study the goal is to observe whether smaller JNPs can induce the same effects independently to the type of cell and therefore to the possibility to activate some specific death-inducing pathways. JNPs could represent a better option respect to the magnetic disks because those latter are too large for tumor tissues penetration and treatment.

Before moving to the hearth of this computational report, the reference idea used as inspiration and relying on the JNPs magnetolytic therapy exposed by *Hu et al.*¹ is briefly summarized hereafter. Fe₃O₄ magnetic nanoparticles (MNPs, 5nm diameter) were mixed together with an inorganic polymer (PS₁₆-b-PAA₁₀) to form JNPs with an average diameter of 180nm. The therapy efficacy was tested in vitro applying a 50 rpm spinning magnetic field for 15 min, in line with the results of *Kim et al.*⁵, to have a mechanical-induced cell death only. Tryphan blue was used to assess cells viability and a reduction of 77% was observed. Figure 2 (b) and (c) illustrate the therapy mechanism.

One of the main advantages of using magnetic JNPs as described by *Hu et al.*¹ is, in addition to the previously described easy and precise control, the low cytotoxicity. This is evident if compared for example to chemotherapies based on drug-carrier nanoparticle. In this case, the presence of a toxic compound could trigger heavy side-effects in off-target tissues. To achieve a low-degree of toxicity, several fabrication techniques and magnetic JNPs compositions have been developed in the last years and some encouraging results were found. *Sotiriou et al.*⁶ demonstrated for example a possible way to manufacture non-cytotoxic, non-sedimenting, non-agglomerating and suspension-stable JNPs. Photostability, described in the next paragraph, and eventually other interesting properties can also be achieved.

Another important advantage compared to nanoparticles-based cancer phototherapies is the absence of generated heat or reactive oxygen singlets⁷ that could generate damages to the nearby healty cells or tissues⁵. Those hyperthermia therapies are based on an heat-induced cellular toxicity induced by the excitation of magnetic nanoparticles with an high frequency oscillating magnetic field. In the proposed magnetolytic therapies, very low frequencies are used, in line with the results found by *Kim et al.*⁵

Methods

To simulate the magnetolytic therapy described by *Hu et al.*¹, dissipative particle dynamics (dpd) simulations are used. The advantage of the dpd method is the relatively large temporal and spatial achievable scale compared to molecular dynamics, thanks to coarse-graining.

In a first phase, some tuning simulations are performed to optimally set-up the parameters. For all the assays a cubic simulation box of 32 units-long edges with density of 3 units and temperature of 1 unit is used. A bilayer lamella composed of dimyristoylphosphatidyl (DMPC) lipids of thickness 5 units is introduced in the center of the z-axis. DMPC are used since they constitute a major component of biological membranes. 3 types of beads are initially created, representing water (W), the membrane lipids heads units (H) and the tail units (T). DMPCs lipids are coarse-grained as $H_3(T_4)_2$ polymers and represents the 1.9050% of all the polymers in the simulation box. The remaining 98.0950% is constituted by the solvent (water). This composition was tuned by some experimental simulations to introduce a surface tension in the membrane (visually assessed with ParaView). This tension is intended to favorize the hypothetical nanoparticle-induced formation of pores and the their "open-state" persistence. The selected membrane is impermeable to the water beads. A visual summary of the tested compositions is provided with Figure 1.

To quantitatively measure the pores formation, the water beads density fluctuations are measured with a dedicated command. The water molecules on the 2 sides of the membrane are differently labeled (top: W; bottom: Wb) and the simulation box is divided along the z-axis in 2 parts. The average number of Wb beads in the bottom part is measured each 100 time-units so that, by knowing the initial number of Wb beads, their flux through the impermeable membrane caused by the formation of some pore can be quantified. To only let the Wb and W beads flow to their opposite side of the simulation box through the membrane and not through the bottom and top walls (because of the presence of periodic boundaries), an impermeable top and bottom barriers are created. To do that, 2 layers of thickness 2 units are defined at the early stages of the simulations (at time-step 100) and the water molecules inside them are freeze. After changing the identifier of those beads (bottom barrier: fixedWb; top barrier: fixedWu), their physical

properties are changed to be strongly repulsive to the W, Wb beads. This set-up was then tested and after 17000 timesteps not a single Wb or W molecule was able to cross those barriers.

To introduce a Janus nanoparticle in the simulation, a spherical volume of water molecules is selected just above the membrane plane. Then, those beads are polymerized to form a single-polymer unit constituting the JNP. Those beads are labeled as NP and are set to be attractive towards the H beads of the membrane lipids. By this way, the affinity for the cancer cells is simulated. The upper-half of the sphere is then selected and the properties of those beads are modified to set them neutral towards the water (W) and the lipid tails (T) beads and slightly repulsive towards the lipids heads (H). This hemisphere represents the magnetic part of the JNP and the beads constituting it are labeled as MP.

The application of an oscillating force simulating the effect of a spinning magnetic field on the magnetic beads is introduced by applying to those latter a constant force in z-direction. This force changes direction each N timesteps (half of the oscillating period). To do that, a custom python script automatically writing a list of commands to the end of the simulation input files was created.

To avoid the crossing of the bottom and top simulation box walls (presence of periodic boundaries), the nanoparticles are set to be strongly repulsive to the 2 layers of fixed water molecules constituting the barriers described above. Moreover, to avoid an excessive nanoparticle deformation when a strong force is applied to them, the Hookean spring constant defining the JNP polymer bonds flexibility was tuned with some tests and set to a very high value of 1700. This extreme value is also useful when the period of oscillation of the force is too high. In this case, the JNP hits the bottom or top walls and, because of the strong repulsion from them, it is blocked on its surface until when the force switches to the opposite direction. If the JNP polymeric bonds stiffness is too low, this latter deforms under the pushing action of the force until becoming completely flat and the beads constituting the 2 hemispheric halves mix together. By accurately tuning all those parameters, a good simulation quality is achieved, as illustrated in Figure 2.

The conservative parameters of all the beads are summarized in Table 1.

The simulation of the magnetolytic therapy initially considers a single janus nanoparticle of radius 2 units, subjected to different oscillating forces amplitudes and frequencies. The tested forces are 20, 50, 100, 150, 200, 300, 350, 400 and for each of them the following half-oscillation period values are tested: 300, 450, 600. The force is applied at timestep 700 and continues until the end of simulation, at timestep 22000. Because the goal is to simulate a membrane disruption and not to measure quantities such as the simulation beads diffusion, it is not important to wait until the membrane equilibrium to apply the force. Snapshots are saved each 10 timesteps to optimally observe the oscillating behavior of the JNP. A summary of all the simulation commands and of their time of application is provided with Table 2.

To convert the measured quantities from the dpd reduced units to real physical values and units, the experimental data measured by *Kučerka et al.*⁸ are used as reference. The reported thickness and single-lipid surface area of an unilamellar DMPC bilayer are respectively 44.5 ± 0.3 Å and 58.9 ± 0.8 Å² at 30 ± 0.1 °C. From this it can immediately be concluded that one dpd temperature-unit corresponds to ~ 30 °C. For a cubic box with edges length L, the following relation holds:

$$a_0 = \frac{(L_{dpd}r_0)^2}{N_{lipids on one side of the bilayer}} \tag{1}$$

From where:

$$r_0 = \sqrt{a_0 \frac{N_{lipids on one side of the bilayer}}{L_{dpd}^2}}$$
 (2)

With r_0 being the real physical value of a simulation box length unit and a_0 the experimentally measured lipid surface area. From the simulations outputs, it can be extracted that 1573 DMPC lipids are present in total. By injecting all the values in (2), we get:

$$r_0 \cong \sqrt{5.9 \frac{1537/2}{32^2}} \cong 2.1 \, nm$$

Alternatively, this conversion can also be done with the membrane thickness using the following formula:

From where:

$$r_0 = \frac{bilayer\ thickness_{real}}{bilayer\ thickness_{dpd}} \cong \frac{4.45}{5} = 0.89\ nm$$

In both cases, this is only a rough approximation of the conversion scale; for the following sections of this project the average between those 2 last values is used:

$$r_0 = \frac{0.89 + 2.1}{2} = 1.495 \, nm$$

Once determined the ideal simulation setup, to identify the real physical properties needed for a JNP to be subjected to a force F under the application of a magnetic field B, the Lorenz force law can be used:

$$\vec{F} = a\vec{v} \times \vec{B}$$

where q is the total charge of the JNP magnetic-half and v its velocity, that can be extracted and averaged from the data used to generate Figure 5. It is important to notice that the magnetic force only depends on the electric charge and not on the mass of the moving nanoparticle! Analogously to the previous procedure, a conversion between the dpd and real-world velocities and forces could be found.

To determine if the presence of more than one JNP enhances the DMPCs bilayer disruption, the configurations displayed in Figure 3 are created. In the case of the triangular conformation (Figure 3a), all the beads are subject to the identical oscillating force. To assess the effect of different applications of the force on multiple beads, the squared conformation is used (Figure 3b). In this case, the 2 beads lying on top of the membrane are initially subjected to a downward force, whether the 2 beads lying on the bottom of the membrane to an upwards force. The magnitude and oscillation period of those forces are the same.

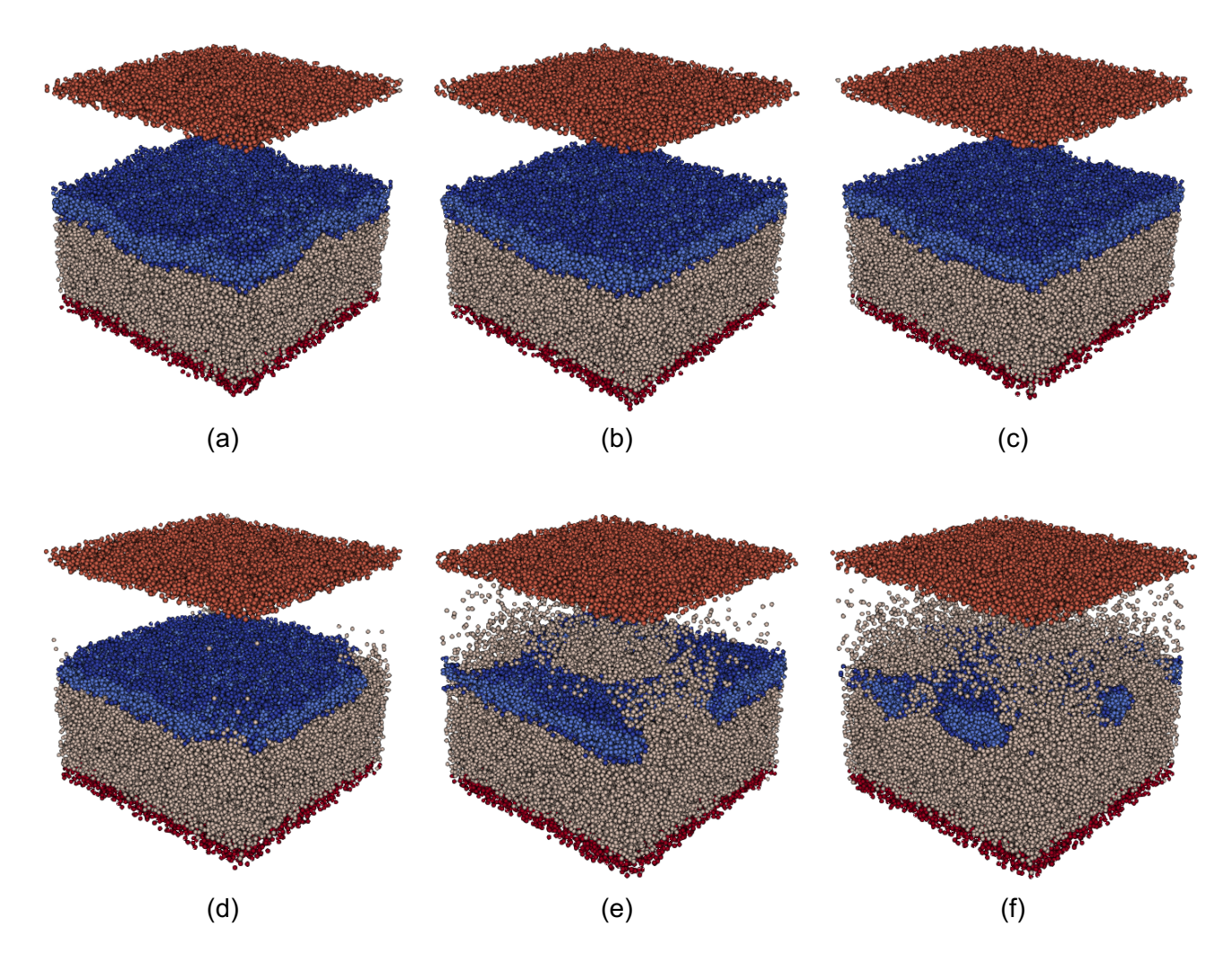


Figure 1 – Snapshots at time-point 16000 (over 17000) of the different simulations performed to tune the membrane lipidic composition. The simulation box bottom-half water molecules as well as the water-barriers (described in the methods) are shown. Orange: upper water barrier; Red: bottom water barrier; Beige: sim-box bottom-half water molecules; Deep-blue: lipid heads beads (H); Light-blue: lipid tails beads(T). The total water/lipid fractions of each assay are the following: (a) Lipid: 0.021013, Water: 0.978987 (b) Lipid: 0.019013, Water: 0.980987 (c) Lipid: 0.01803, Water: 0.98197 (d) Lipid: 0.01503, Water: 0.98497 (e) Lipid: 0.01203, Water: 0.98797 (f) Lipid: 0.00903, Water: 0.99097

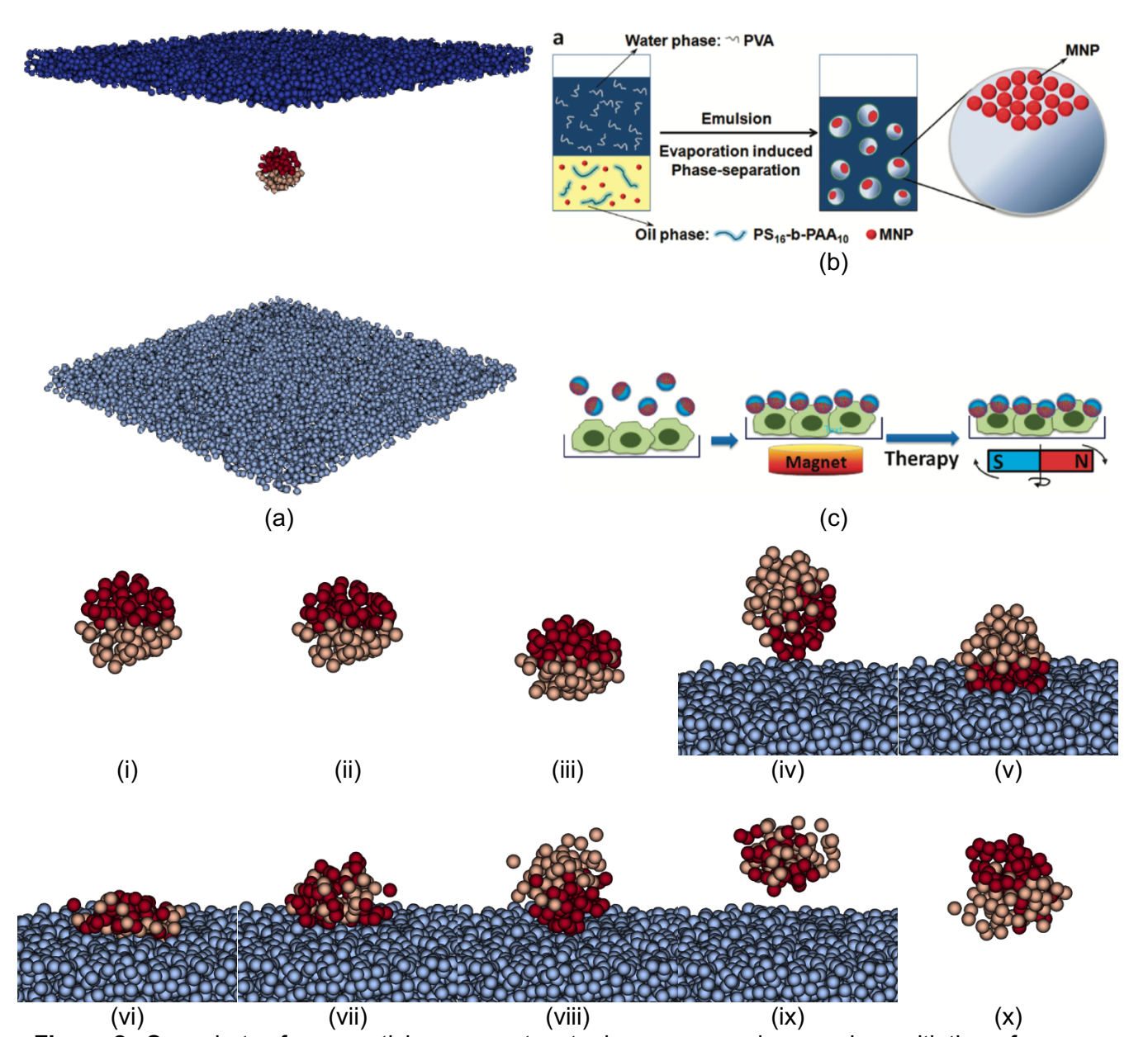


Figure 2 - Snapshots of nanoparticles parameters tuning assays and comparison with the reference paper JNPs illustrations. **Top**: (a) Snapshot of a janus nanoparticle (JNP) of radius 2 units at the moment of initialization. The bottom and top water barriers are shown as well in blue. Red: magnetic beads; Orange: cancer-cell affine beads (beads affine to H-beads of membrane, not shown here). (b) *Hu et al.*¹ JNP fabrication and composition diagram (adapted figure). MNP = magnetic NanoParticle; PS₁₆-b-PAA₁₀ = an inorganic polymer (c) *Hu et al.*¹ application of JNP in the magnetolytic cancer therapy. **Bottom**: sequence of snapshots showing the application of a very intense oscillating force to the magnetic half of a JNP. Magnitude of the force: 300; half-period of the force: 300 time units. (i) Prior force application; (ii) 10 time units after the downward force application. Until (iii), a compression of the JNP can be observed; (iv) Because of the force applied downwards on the red beads, the JNP has rotated by 180°; (v)-(vii) the JNP hits the bottom wall and slightly bounces back. The applied force is still downwards, since less than 300 time units have passed from the moment of the initial force application; (ix) The force is now upward and always applied to the red beads, the JNP deforms; (x) After a while a rotation of 180° is observed as described before and the deformation is reduced. The JNP is still pulled upwards.

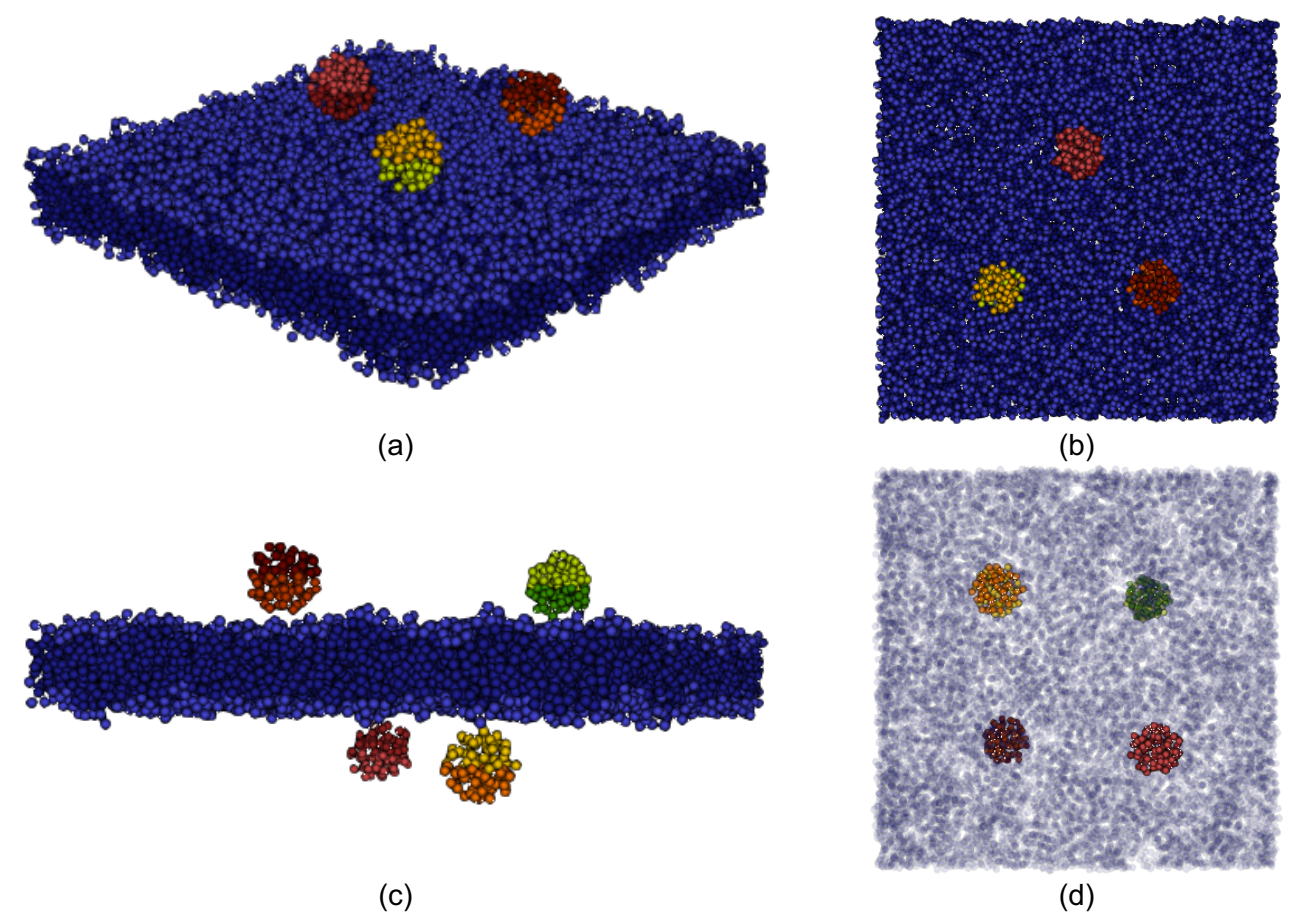


Figure 3 – Snapshots of the configurations of the multiple-JNPs simulations at the moment of the nanoparticles inizialization. (a, b) 3 JNPs of radius 2 units are disposed on the corners of an equilateral triangle of edge 12 units; (c, d) 4 JNPs of radius 2 units are placed on the corners of a square of edge 12 units. The JNPs on the 2 diagonals are placed under or over the membrane plane and the applied force is then initially directed respectively towards the top or the bottom of the simulation box; (a, b, c, d) In all the cases, the membrane-affine half of the JNPs is initially oriented towards the membrane and the magnetic-half on the opposite direction.

	Н	Т	W	Wb	FixedWb	FixedWu	NP	MP
Н	30							
Т	35	10						
W	30	75	25					
Wb	30	75	25	25				
FixedWb	30	75	100	100	25			
FixedWu	30	75	100	100	100	25		
NP	15 (low affinity) 10 (high affinity)	35	25	25	5000	5000	25	
MP	25	35	25	25	5000	5000	25	25

Table 1 – Summary of the conservative parameters between all the beads in the simulations. Units in terms of k_BT/r_0^2 .

Time	Commands
0	Start of the simulations.
100	Creation of the water-repellent bottom and top walls, labelling of Wb, FixedWu, FixedWb beads and definition of their physical properties.
600	Start of beads density fluctuation measurements; creation of the JNPs, labelling of MP, NP and definition of their physical properties.
700-	Periodically, each N timesteps application of a downwards z-oriented force on the MP beads
22000	of the JNPs, followed by an application of an upwards force.
22000	End of the simulations.

Table 2 – Summary of the time of application of all the commands constituting the simulations.

Results and discussions

The usage of dpd-simulations to investigate the effects of a magnetolytic therapy on the disruption of a cancer cell membrane presents some technical restrictions. In fact, compared to the therapy set-up applied by the authors of the reference paper 1, some spatial and temporal limitations imposed by the computational power are present. Firstly, for what it concerns the JNPs size, it was impossible to simulate spheres with 180nm of diameter. According to the previously computed unit-scale this would have required nanoparticles of an approximative radius of $180/1.495 \sim 120$ simulation box units, clearly too large to be reasonably simulated. Secondly, the few-seconds timescale of the oscillating magnetic field (few Hz time scale) is impossible to achieve with dpd. At the best, only few microseconds can in fact be efficiently simulated.

Beside those limitations, it is interesting to observe the effect of smaller JNPs on the cellular membranes. In case of an efficient membrane disruption observation, because of their reduced size this could result in very interesting clinical. This could in fact potential be associated with a better tumor-tissue penetration.

From the output simulation files, Figures 4 and 5 are created. In Figure 5 it is clearly visible the time-periods where JNPs are blocked towards the membrane if the force oscillating half-period is too large. The top 10 time-points and associated parameter combinations exhibiting the maximum Wb water flux between the bottom and the top half of the simulation box are summarized in Table 3. Those are the conditions where a maximal membrane disruption is expected to be observed. Only the top negative Wb average losses over 100 time-periods are reported. This means that the Wb leaves the bottom half of the simulation box to flow towards the top-half. To verify the formation of some pores, Figure 6 was created with ParaView for the simulation with a force of amplitude 400 units, a half-oscillation period of 300 units and a JNP with an high affinity for the cellular membrane. This is the fact optimal candidate in terms of parameters combination, allowing the maximal membrane disruption, since 3 of the first 4 time-points of Table 3 timepoints belong to this simulation.

To assess the disruptive power of multiple JNPs, the optimal force half-period and amplitude parameters are applied on the beads configurations of Figure 3. Results are reported in Figures 7 and Table 4. From Figure 7 it is clearly visible for the square-conformation the previously described alternating oscillation of the JNPs in the opposite z-directions. By simply comparing Table 3 with Table 4 and Figure 4 with Figure 7, it can be immediately observed that, when more than one JNP is present, the Wb leaks are much more significant and occur earlier in the simulation. From Figure 7 it can also be observed that the square conformation is associated to a greater Wb diffusion from the bottom to the top halves of the simulation box. This configuration could however be difficult to achieve in vivo because of the initial positions of the JNPs on the 2 opposite sides of the membrane. A dedicated study should be carried on to determine the feasibility of this approach. The membrane disruption is also visually assessed with ParaView. The rendered animations are available in the supplementary materials. Some artifacts due to the periodic simulation box boundaries seems to be present but the overall quality of the simulation is good. To avoid those problems, a larger box could for example be used.

For a future study, it would be interesting to test more JNPs geometrical conformations and sizes. It could also be interesting to determine if the rotation of the beads observed and described in Figure 2 has a role in the membrane disruption.

Conclusions

With this short report the efficacy of the proposed magnetolytic cancer therapy was demonstrated and confirmed. From the simulations it seems that an efficient membrane disruption can be achieved independently to the activation of some intrinsic cellular pathways as was initially suggested and reported by *Kim et al.*⁵. The mechanism of action could therefore only depend on a magnetomechanical effect. The suggestion (not empirically tested) of *Hu et al.*¹ to biofunctionalize the magnetic JNPs to make them affine to the cancer cells was implemented and tested. This revealed out to be very efficient. The simulations should be repeated with non-biofunctionalized beads to compare the effects. The membrane disruption was observed for shorter timescales and with smaller beads compared to what *Hu et al.* reported. This presents several advantages in terms of in-vivo applications, as discussed in the text. More simulations are however needed to robustly assess the best parameters yielding to the optimal treatment efficacy. With those data, JNPs can then be manufactured to satisfy all the needed physical properties, always considering all the biological limitations. For example the charge of the JNPs has to be adapted so that the application of a non-toxic magnetic field is sufficient to ensure the induction of a certain pre-determined

electromagnetic force. The main limitation of this report was the computational power: with over 84 hours of total simulation time, only certain aspects could have been tested.

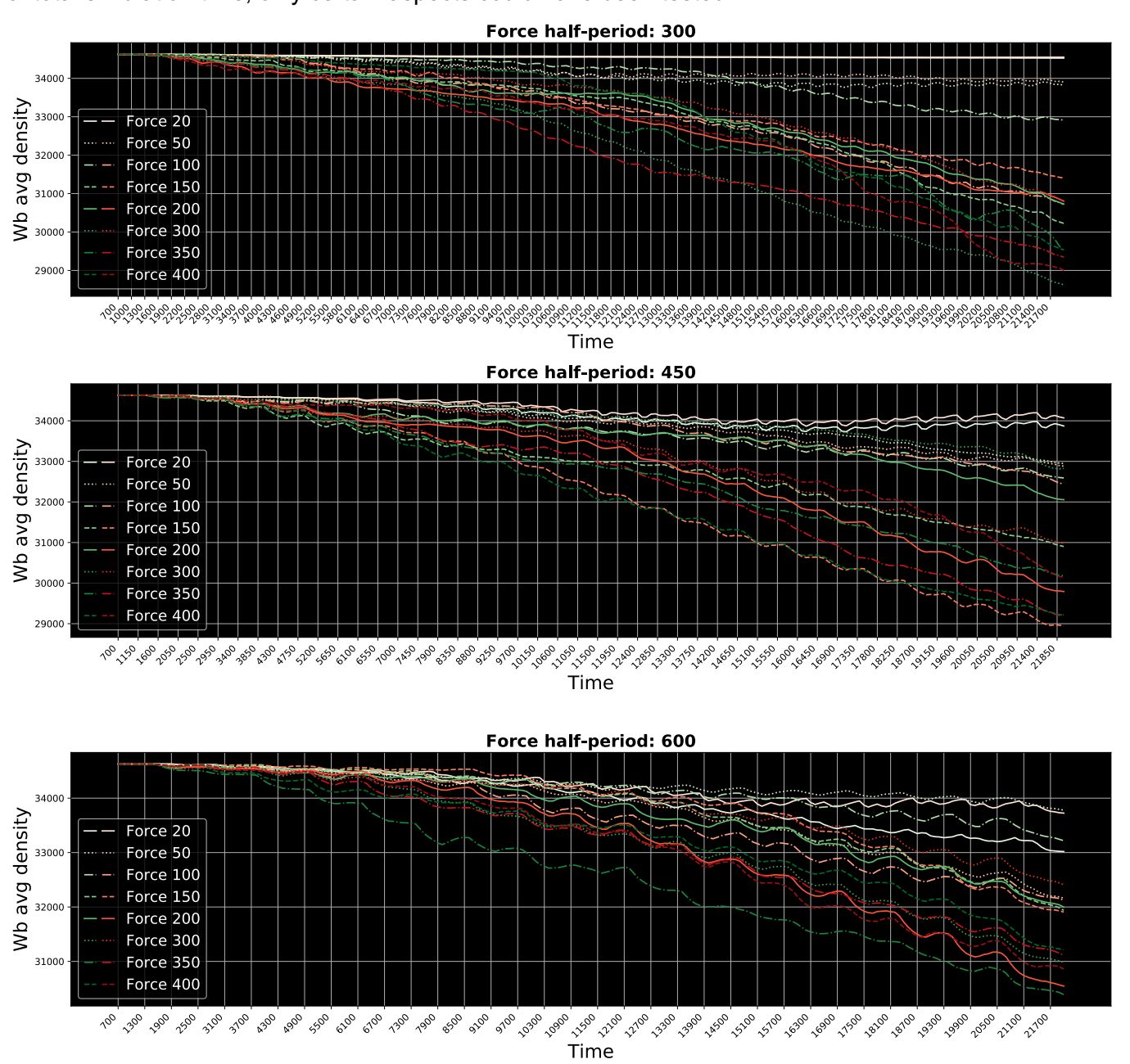


Figure 4 – Average number of Wb number (Wb "density") in the bottom-half of the simulation box for all the simulations from the time of the force application on the single JNPs (700 time units). The simulations are grouped by the oscillating force half-period, reported in the figure titles and set as spacing for the vertical grid lines. The green and red colormaps are assigned to the low- and high-affinity simulations respectively (JNP-membrane affinity). A black background is used to enhance the visualization.

time- step	avg Wb density	difference	force period	force amplitude	JNP membrane affinity
21900	29634.7	-176.5	300	350	low
19700	30035.5	-133.3	300	400	high
17400	31191.1	-131.5	300	400	high
19800	29906.7	-128.8	300	400	high
21500	33853.5	-127.2	450	20	low
21500	34073.5	-123.6	450	20	high
19600	31320.4	-123.4	600	200	high
19200	30792.9	-123.1	300	350	low
21800	29811.2	-121.2	300	350	low
20800	30963.1	-119.6	600	200	high

Table 3 – Top 10 highest Wb "density" (number) variations for the single-JNPs simulations. The difference represents the average loss (flux) of Wb beads from the bottom-half of the simulation box towards the top-half over the previous 100 time-points at the time-point indicated in the time-step column. Colors indicate the values coming from the same simulations.

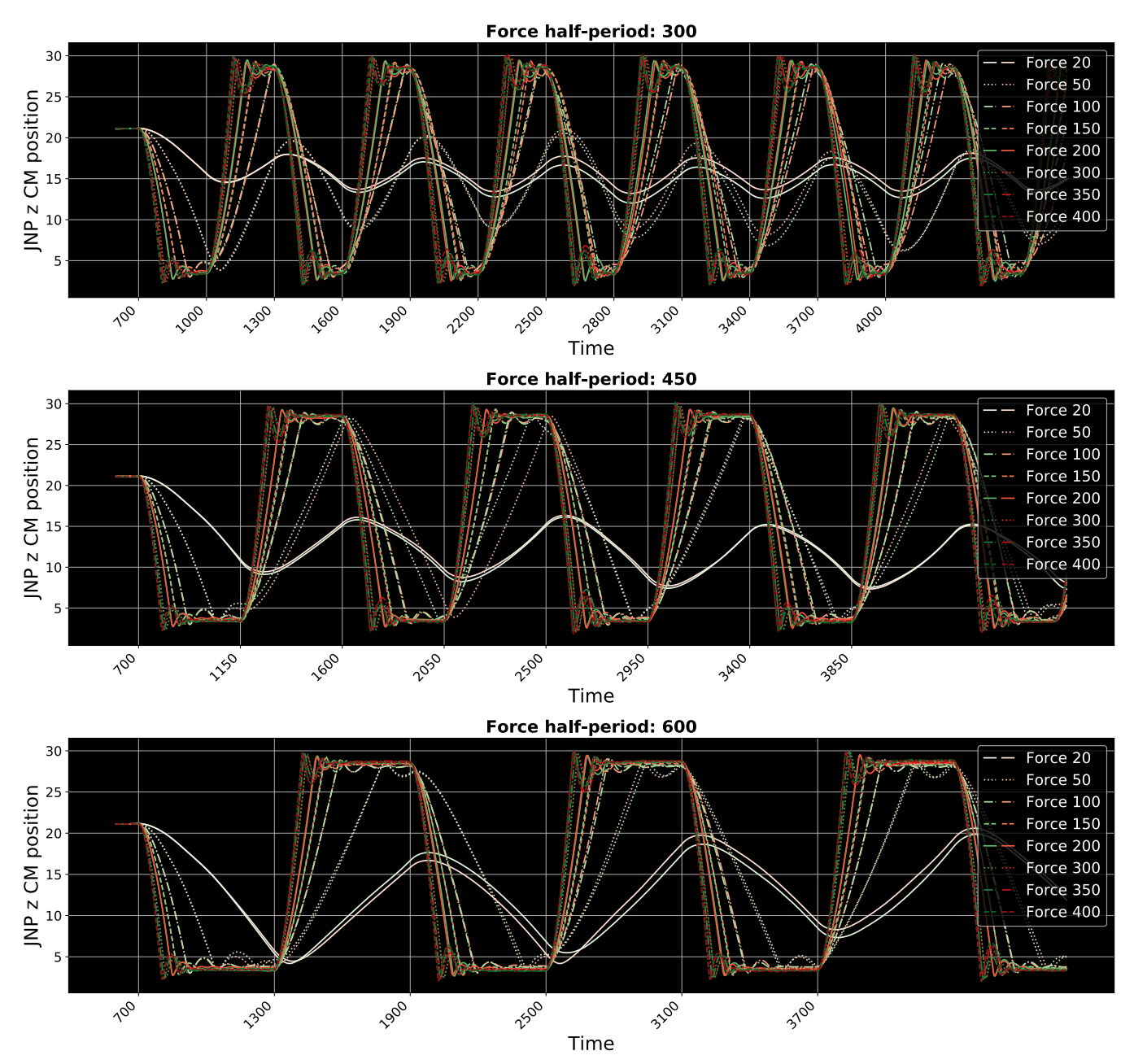


Figure 5 – JNP center of mass z-position in simulation box length units for all the single-JNP simulations from the time of the force application (700 time units). The simulations are grouped by the oscillating force half-period, reported in the figure titles and set as spacing for the vertical grid lines. Only the first 6 half-periods are displayed; the behavior is very similar also for the following timepoints. The green and red colormaps are assigned to the low- and high-affinity simulations respectively (JNP-membrane affinity). A black background is used to enhance the visualization.

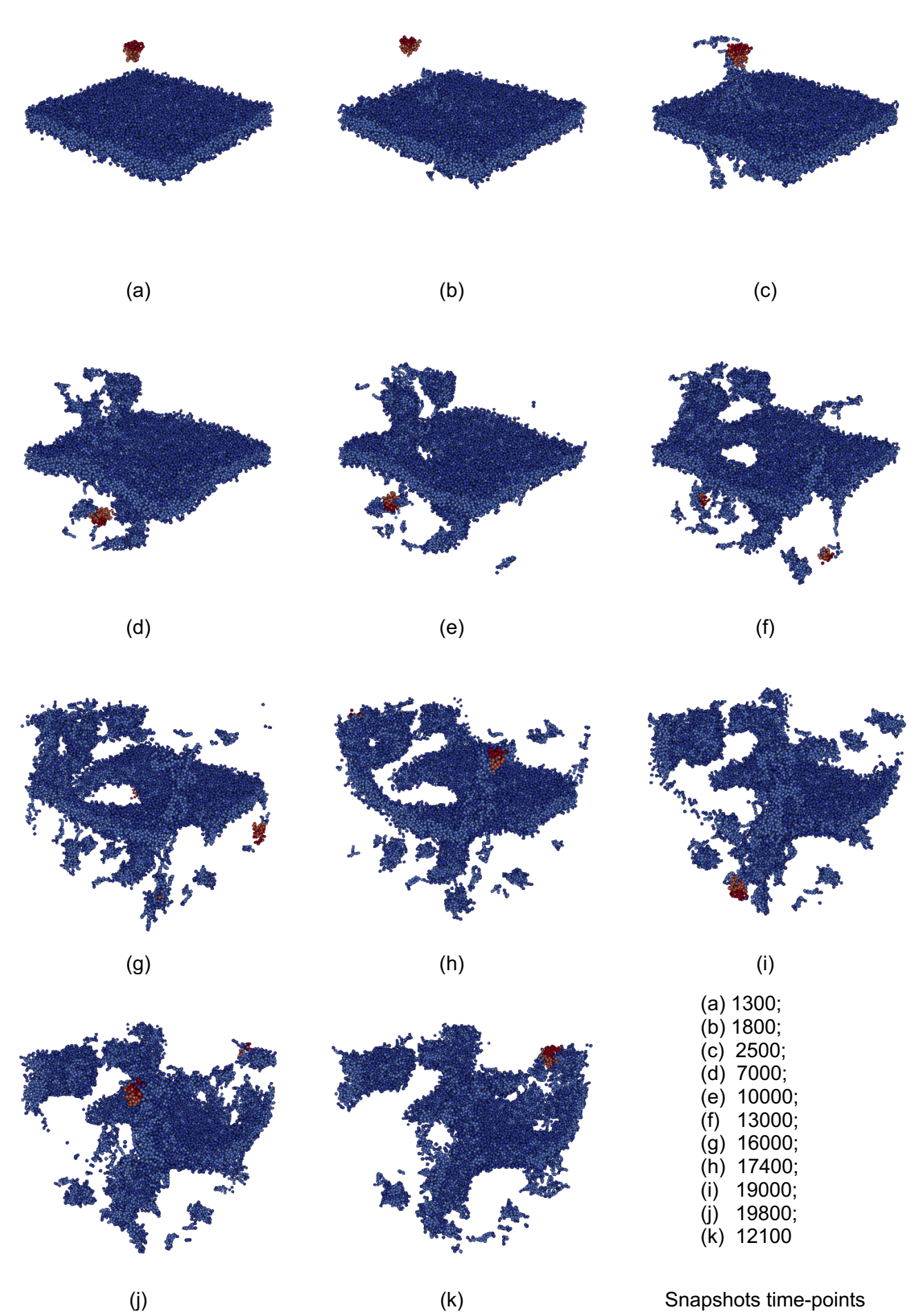


Figure 6 – Snapshots at several timepoints of the single JNP simulation with an applied oscillating force of magnitude 400, half-period 300 time units and high affinity for the membrane. The magnetic half of the JNP is displayed in red, the membrane-affine half in orange. The water molecules are not showed.

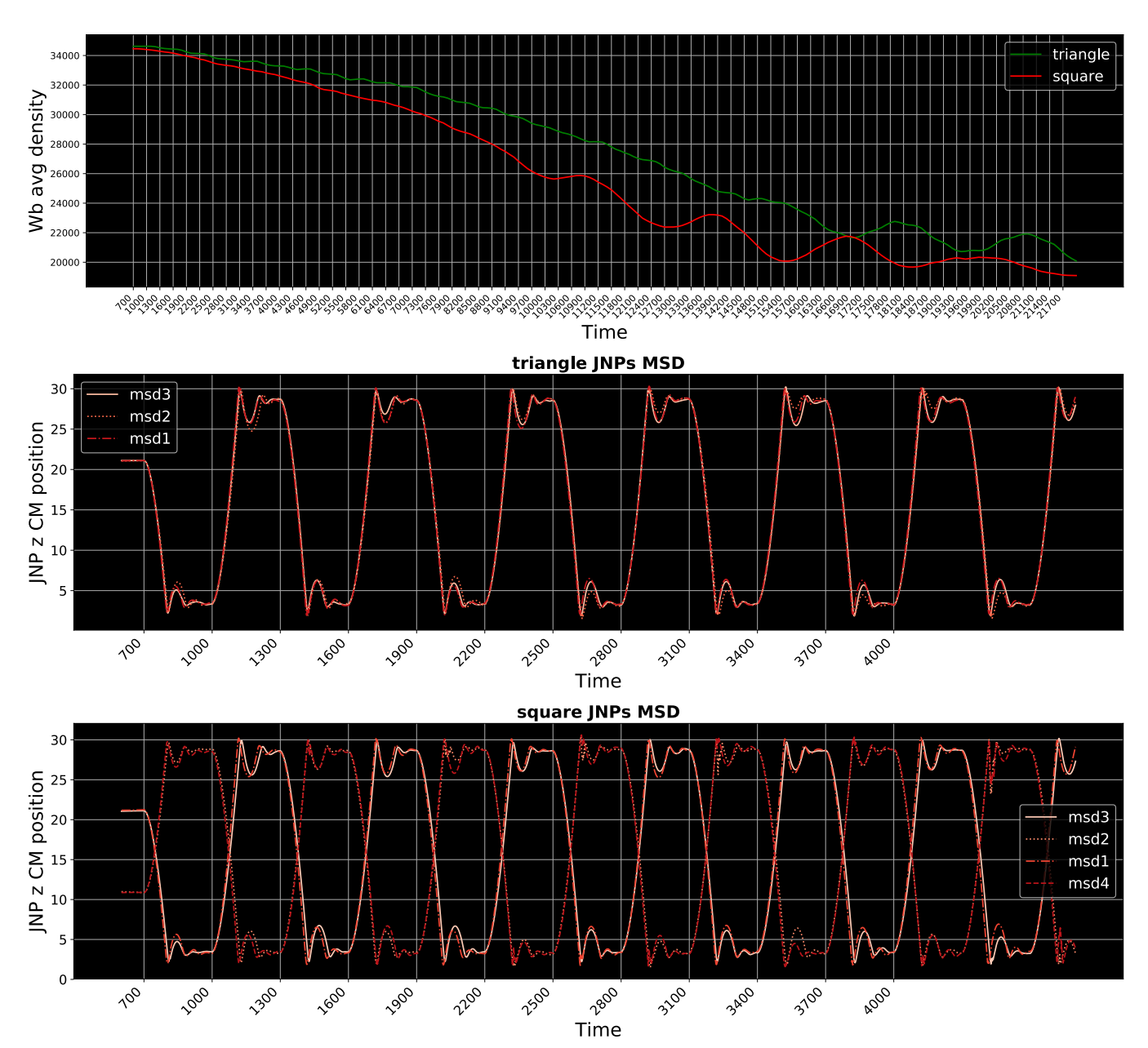


Figure 7 – Multiple JNPs simulation results. Applied oscillating force: amplitude 400, half-period 300; JNP highly affine for the membrane. **First panel**: average number of Wb number (Wb "density") in the bottom-half of the simulation box for all the simulations from the time of the force application (700 time units) on the single JNPs. **Second and Third panels**: JNPs centers of mass z-positions in simulation box length units for the triangle and square configurations simulations from the time of the force application. The oscillating force half-period (300 time units) is set as spacing for the vertical grid lines. Only the first 6 half-periods are displayed; the behavior is very similar also for the following timepoints. The different curves corresponds to the different JNPs present in the simulations.

conformation	time- step	avg Wb density	difference	force period	force amplitude	JNP membrane affinity
triangle	11900	23800.4	-287.9	300	400	high
triangle	11800	24088.3	-282.4	300	400	high
triangle	9400	26838.9	-275.5	300	400	high
triangle	12100	23262.5	-275.4	300	400	high
triangle	11700	24370.7	-268.7	300	400	high
square	11900	23800.4	-287.9	300	400	high
square	11800	24088.3	-282.4	300	400	high
square	9400	26838.9	-275.5	300	400	high
square	12100	23262.5	-275.4	300	400	high
square	11700	24370.7	-268.7	300	400	high

Table 4 – Top 5 highest Wb "density" (number) variations for the triangle and square-conformations multi-JNPs simulations. The difference represents the average loss (flux) of Wb beads from the bottom-half of

the simulation box towards the top-half over the previous 100 time-points at the time-point indicated in the time-step column.

Bibliography

- 1. Hu, S.-H. & Gao, X. Nanocomposites with Spatially Separated Functionalities for Combined Imaging and Magnetolytic Therapy. *J. Am. Chem. Soc.* **132**, 7234–7237 (2010).
- 2. Shao, D. *et al.* Janus "nano-bullets" for magnetic targeting liver cancer chemotherapy. *Biomaterials* **100**, 118–133 (2016).
- 3. Le, T. C., Zhai, J., Chiu, W.-H., Tran, P. A. & Tran, N. Janus particles: recent advances in the biomedical applications. *Int. J. Nanomedicine* **14**, 6749–6777 (2019).
- 4. Greish, K. Enhanced Permeability and Retention (EPR) Effect for Anticancer Nanomedicine Drug Targeting. in *Cancer Nanotechnology: Methods and Protocols* (eds. Grobmyer, S. R. & Moudgil, B. M.) 25–37 (Humana Press, 2010). doi:10.1007/978-1-60761-609-2 3.
- 5. Kim, D.-H. *et al.* Biofunctionalized magnetic-vortex microdiscs for targeted cancer-cell destruction. *Nat. Mater.* **9**, 165–171 (2010).
- 6. Sotiriou, G. A. *et al.* Hybrid, Silica-Coated, Janus-Like Plasmonic-Magnetic Nanoparticles. *Chem. Mater.* **23**, 1985–1992 (2011).
- 7. Zhang, Y., Huang, K., Lin, J. & Huang, P. Janus nanoparticles in cancer diagnosis, therapy and theranostics. *Biomater. Sci.* **7**, 1262–1275 (2019).
- 8. Kučerka, N., Kiselev, M. A. & Balgavý, P. Determination of bilayer thickness and lipid surface area in unilamellar dimyristoylphosphatidylcholine vesicles from small-angle neutron scattering curves: a comparison of evaluation methods. *Eur. Biophys. J.* **33**, 328–334 (2004).